

Zeolite structural investigations by high resolution solid state MAS NMR (magic angle spinning nuclear magnetic resonance)

G.T. Kokotailo*, C.A. Fyfe*, G.J. Kennedy, G.C. Gobbi, H. Strobl, C.T. Pasztor, G.E. Barlow and S. Bradley

Guelph-Waterloo Centre for Graduate Work in Chemistry, Guelph Campus, Department of Chemistry and Biochemistry, University of Guelph, Guelph, Ontario, Canada N1G 2W1

W.J. Murphy and R.S. Ozubko

Esso Petroleum Canada, Research and Engineering Department, Sarnia, Ontario, Canada. N7T 7M1

Abstract - A number of techniques including single crystal and powder X-ray diffraction methods, IR, XPS, electron microscopy and neutron diffraction have been used to characterize zeolites. This paper discusses the adaptation of another method, solid state MAS NMR, for obtaining high resolution ^{29}Si and ^{27}Al spectra and thus establishing the local environments of these nuclei and how they are affected by sorbed molecules, temperature, defects and distortion. The ability to obtain high resolution spectra by the use of novel dealumination techniques has made it possible to identify atomic sites and together with X-ray data provides a more complete description of the structures of zeolites.

INTRODUCTION

Zeolites are an important class of materials which are widely used as sorbents, ion exchangers, catalysts and catalyst supports (1 - 4). The unique feature of zeolites, which are framework structures with uniform pore systems, is their selective accessibility to sorbates and reactant molecules. They control the size of the molecule adsorbed and the size of the reaction product. Catalytic activity is characteristic of the zeolite and is dependent on the size and geometry of its channel system, the composition of the framework, the distribution of T-atoms in the unit cell and in the crystal, the nature, distribution and mobility of adsorbed atomic and molecular species and cations and also the presence of strains and defects.

A number of techniques have been used to characterize zeolites. The unavailability of good large crystals especially of synthetic zeolites has led to the use of powder diffraction techniques to resolve their structures. One of these techniques consists of model building followed by DLS refinement (5) and simulation of a Smith plot (6). Several structures have been solved by this method: ZSM-5 (7), ZSM-11 (8), ZSM-12 (9), ZSM-22 (10), ZSM-23 (11) and ZSM-39 (12). An alternative method of evaluating trial structures by generating Fourier projections from experimental intensities has resulted in the determination of the structure of Theta-1 (13). There are a number of reviews dealing with various aspects of zeolite structures (1, 4, 14, 15).

The knowledge of zeolite structures is limited, however, although the topology or general features of the frameworks of a large number of zeolites are known. The cation, water and organic molecule sites are known for only a few zeolites. The Si and Al sites may be distinguished by the difference between the T-O bond length (Si-O = 1.62 Å and Al-O = 1.73 Å) if there is long range Si and Al ordering throughout the crystal although this is seldom true. ZSM-5 crystals tend to grow with a high Al content outer shell (16) while zeolite Y has a higher Si concentration on the surface (17). It is also not known whether Al occupies certain sites preferentially and whether some of it is not in the framework.

The determination of cation sites has been reviewed by Mortier (18). The Rietveld X-ray powder profile method for refining structures (19) has been applied (20). Tunable monochromatic synchrotron radiation in conjunction with this technique was used to refine the structure of zeolite A (21) and the use of a neutron source has made it possible to identify OH groups (22). X-ray photon spectroscopy has been employed to determine the composition of surfaces (23).

Considerable effort has been expended to resolve the presence and nature of defects in zeolites. Bennett and Gard (24) were the first to detect stacking faults in the erionite-offretite family with electron diffraction techniques. Contrast lines in transmission electron microscopy indicated the presence and concentration of stacking faults in erionite (25) and ZSM-4 (26). X-ray powder diffraction was used to detect the presence of stacking faults in the pentasil family (27). Cowley's pioneering work established an electron microscope technique for lattice imaging which was adapted to determine faulting in zeolites and has been reviewed by Thomas (28).

This paper describes the adaptation of solid state MAS NMR for obtaining high resolution ^{27}Al and ^{29}Si spectra and establishing the local environment of the T-atoms and how the spectra are affected by sorbed molecules, distortions, faults and temperature. The greatly improved resolution in the spectra of highly siliceous analogs makes it possible to index individual atomic sites for zeolites with multiple independent atoms.

HIGH RESOLUTION SOLID STATE NMR (ref. 29)

The NMR spectra of solids with abundant nuclei (eg. ^1H and ^{19}F) are usually broad and featureless due to the dominance of direct dipole-dipole interactions whereas in solution these dipolar interactions are averaged to zero due to rapid thermal motion resulting in high resolution spectra. The situation is simplified considerably by "diluting" the nuclei in the solid matrix either by low isotopic abundance or by physical dilution. With dilution, the homonuclear dipolar interactions between the "dilute" nuclei which drop off very rapidly with internuclear distance become negligible. Heteronuclear dipolar interactions between protons and nuclei in the dilute system can be removed by application of high proton decoupling fields. The remaining interaction is due to the chemical shielding of the nucleus by the surrounding electrons and since this is three dimensional, the chemical shift will be anisotropic (i.e. dependent on the orientation of the nucleus with respect to the magnetic field). The chemical shift anisotropy, H_{CSA} is observed as a broad signal due to the random orientation of crystallites. This pattern can be averaged by "magic angle" spinning (30) of the sample at $54^\circ 44'$ as illustrated in Fig. 1a, giving the isotropic chemical shift similar to that produced by random motion in solution. In addition, cross polarization is used to enhance the dilute nucleus magnetization from that of protons in the system (31). The combined techniques of dipolar decoupling, cross polarization (CP) and magic angle spinning (MAS) yield high resolution spectra for dilute nuclei in the solid state (32).

Since there are no protons covalently bonded to the zeolite lattice, high field proton decoupling is unnecessary, and cross polarization is not possible reducing the experiment to one of MAS alone.

Before discussing specific applications of NMR studies of zeolites, it must be emphasized that NMR and other techniques, especially X-ray diffraction, are complimentary. NMR chemical shifts reflect the local magnetic environments and ordering of nuclei while X-ray diffraction reflects long range ordering. Their combined use provides a much more complete description of the framework structure of these materials, than either technique alone.

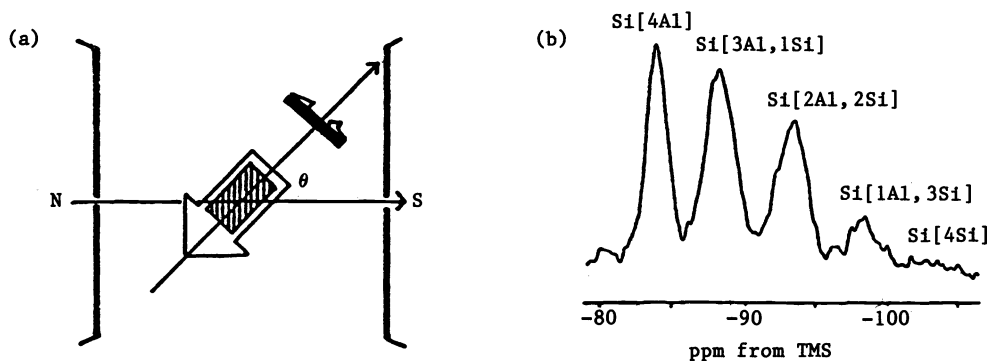


Fig. 1 a) Schematic representation of the MAS experiment; Affect of spinning on the chemical shift anisotropy; $H_{\text{CSA}} = (\cos^2\theta - 1)$ (other terms) $+ 3/2 \sin^2\theta \sigma_{\text{AVE}}$. If $\theta = 54^\circ 44'$, $\sin^2\theta = 2/3$ and $(3\cos^2\theta - 1) = 0$ so $H_{\text{CSA}} = \sigma_{\text{AVE}}$

b) ^{29}Si MAS NMR spectrum of zeolite analcite showing the five possible silicon environments.

LOW SILICA ZEOLITES

Since Lippmaa's (33) early work there have been a number of NMR investigations of low Si/Al zeolites which have been reviewed (34). In general for ^{29}Si MAS NMR spectra of a zeolite with one independent atom and $\text{Si}/\text{Al} > 1$ Lippmaa showed that the spectra were sensitive to the local silicon environment, that is to the distribution of Si and Al in the first coordination sphere of the Si atom: Si(4Al), Si(3Al, 1Si), Si(2Al, 2Si), Si(3Al, 1Si) and sensitivity to the local environment. The chemical shift ranges of these 5 peaks for different zeolites are shown in Fig. 2a. From the relative intensities of these five lines the Si/Al ratio can be directly calculated using Eqn. (1)

$$\left(\frac{\text{Si}}{\text{Al}}\right)_{\text{NMR}} = \frac{\sum_{n=0}^4 I_{\text{Si}(n\text{Al})}}{\sum_{n=0}^4 0.25 I_{\text{Si}(n\text{Al})}}$$

If there is more than one independent atom in the framework the interpretation of the spectra may be much more complex (35) and considerable care must be taken in these experiments.

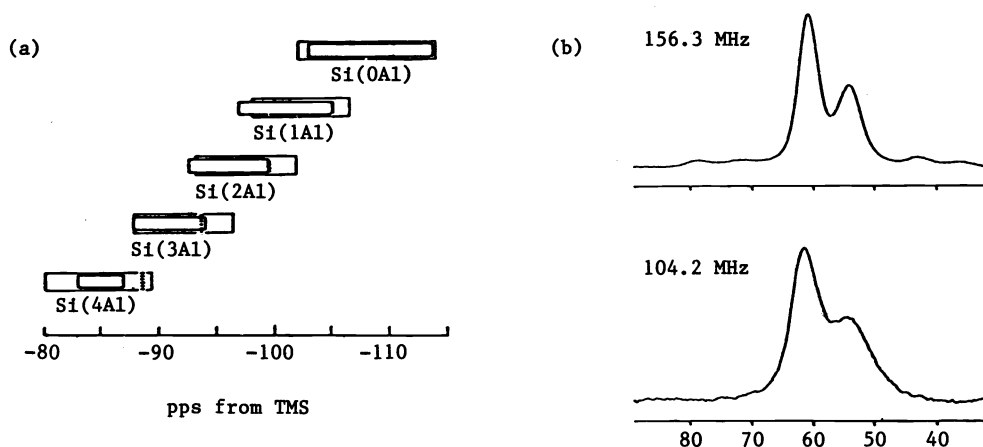


Fig. 2 a) ^{29}Si chemical shift ranges of the five possible local Si environments in the zeolite. The inner rectangles represent the original data of Lippmaa et al. (33)

b) ^{27}Al MAS NMR at 156.3 MHz (9.4T) and 104.2 MHz (14.1T) of zeolite omega.

IMPROVED RESOLUTION OF ^{27}Al SPECTRA AT HIGH FIELDS

The resolution of the two ^{27}Al lines in the spectrum of the zeolite omega is considerably improved when obtained at a 14.1 T field (^1H 600 MHz) compared to that at 9.4 T (^1H 400 MHz) as seen in Fig. 2b (35) and the ratio of the two lines is 1.6:1. The omega structure has 24 T_1 and 12 T_2 sites. This clearly indicates that there is not a random distribution of Al in the omega framework (35). The second order quadrupole effects contribute to the line broadening and asymmetry and vary inversely with the magnetic field. Thus high magnetic fields are essential to obtain "high resolution" ^{27}Al MAS NMR spectra in the solid state.

STUDIES OF HIGH Si/Al ZEOLITES

There are two likely contributing factors to line broadening in ^{29}Si spectra of zeolites: unaveraged dipolar interactions between ^{29}Si and ^{27}Al and distributions of local environments. To determine which of these two line broadening mechanisms is operative MAS NMR spectra at 9.4 T of low Si/Al (<10) and correspondingly high Si/Al (>100) analogs were obtained for a number of different zeolites, of which the spectra in Fig. 3 for mordenite are representative.

Dealumination by treating with water vapour at high temperatures was first described by Kerr (36). A modification of this method (35) was used to obtain very high Si/Al zeolites. The line widths for the low Si/Al zeolites is surprisingly large. From Fig. 3 it can be seen that removal of Al from the framework and replacing it with Si reduces the line width to ~ 1 ppm indicating that Al is responsible for the line broadening. Not only do the line widths diminish but there is a shift to higher fields, to the extreme of the Si(4Si) peak. This indicates that the linewidth is due to a distribution of local environments arising from a change in composition of the second and further coordinating spheres. Thus it is not how much Al is in the lattice but how it is distributed. This is confirmed by the ^{29}Si MAS NMR spectra of a variety of gem-quality minerals, zeolite A, ZK-4 and a highly dealuminated ZK-4. Zeolite A is thermally unstable but the ZK-4 sample was dealuminated by passing water vapour over it at 700° C and atmospheric pressure for 48 hrs (37). The single peak in Fig.

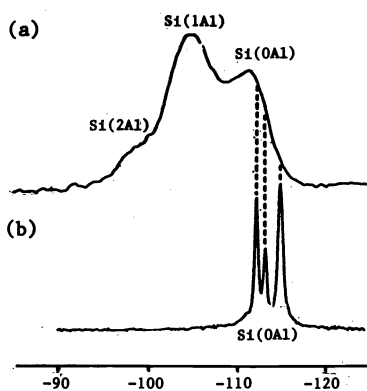


Fig. 3 ^{29}Si MAS NMR (9.4T) of (a) low Si/Al and (b) highly dealuminated mordenite

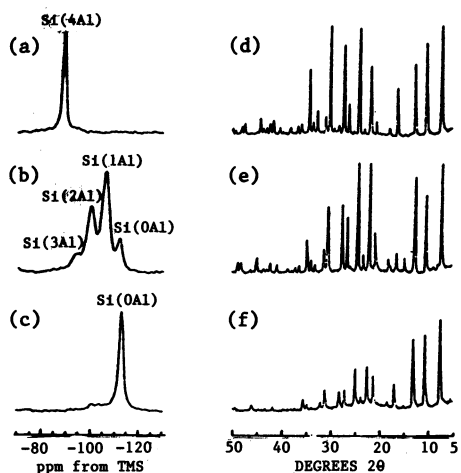


Fig. 4 ^{29}Si MAS NMR (9.4T) of (a) zeolite A (b) ZK-4 (c) completely siliceous zeolite A (d-f) and corresponding XRD powder patterns.

4a is sharp and is due to Si (4Al). For ZK-4, Si/Al > 1, there are five peaks which are broader than the Si (4Al) peak in zeolite A indicating the effect of local environment distribution, Fig. 4b. With dealumination only the Si (4Si) peak appears in Fig. 4c and it is sharp and shifted upfield. The corresponding XRD patterns indicate that the integrity of the framework was preserved.

INTERPRETATION OF ^{29}Si MAS NMR SPECTRA OF ZEOLITES WITH CRYSTALLOGRAPHICALLY INEQUIVALENT SITES

The ^{29}Si MAS NMR spectrum of a low Si/Al mordenite is broad and essentially featureless. Dealumination yields a high resolution spectrum (38) consisting of three peaks with relative intensities of 2:1:3, Fig. 3, compared to the 2:1:1:2 intensity ratios predicted from the mordenite structure which has 16T₁, 16T₂, 8T₃, and 8T₄ sites. Using the average secant of the TOT angles or the average T-T distances the assignment 16T₁, 8T₄, 24(T₂ + T₃) may be made.

Zeolite KZ-2 synthesized according to Parker and Bibby (39) has an XRD pattern similar to those of ZSM-22 (10) and theta-1 (13). The ^{29}Si MAS NMR spectrum, Fig. 5a of a highly dealuminated sample exhibits four lines at -110.87, -112.82, -113.07 and -114.33 (40). The relative intensities are 2:1:1:2 consistent with the proposed lattice structure. Using average T-T distances and TOT angles as determined by Liebau (41) the assignments are T₃, T₁, T₂, T₄.

The ^{29}Si MAS NMR spectrum (40) of highly dealuminated ZSM-12 shows (42) seven well resolved resonances with equal intensity, consistent with the seven independent atoms proposed for the

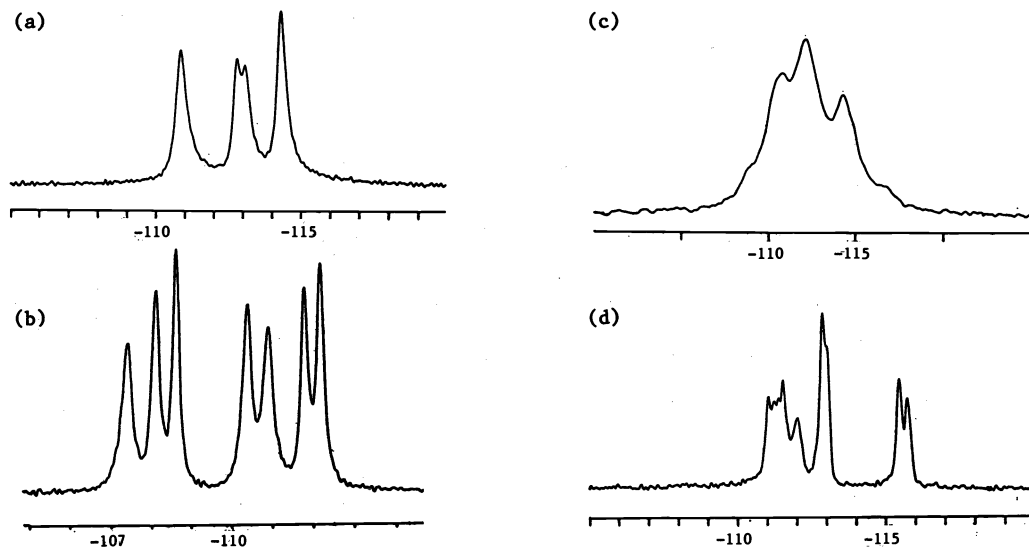


Fig. 5 ^{29}Si MAS NMR (9.4T) of highly dealuminated (a) zeolite KZ-2 (b) ZSM-12 (c) ZSM-23 (d) NU-2 (Beta)

ideal framework (9) (Fig. 5b). There is some discrepancy between the simulated and experimental diffraction patterns, (9) which may be due to an intergrowth of two species. Using average T-T distances derived from the structure data (9) the assignment T_2 , T_4 , T_3 , T_1 , T_5 , T_6 , T_7 for this sample can be made. The structure is being refined using synchrotron radiation and the Rietveld method. A well resolved spectrum of a dealuminated ZSM-23(43) sample could not be obtained, Fig. 5c. The proposed ideal structure of ZSM-23 indicates a Pmmn space group with 4(T_1 , T_2 , T_3 , T_6 , T_7) and 2 (T_4 , T_5) atoms in the unit cell. The number of lines and the ratio of their intensities indicates that T-atom assignments cannot be made and suggests an intergrowth or a variation in stacking sequence.

Zeolite NU-2 (44), a material whose XRD pattern is consistent with zeolite beta (45), was highly dealuminated. Its ^{29}Si MAS NMR spectrum shows nine distinct peaks as seen in Fig. 5d. This should help determine the number of independent atoms in the unit cell and aid in the determination of the structure.

STACKING SEQUENCES

The frameworks of offretite and erionite, are the end members of a family of zeolites, which vary only in the sequence of AA, and AB stacking of layers of cancrinite cages. Random rotation of layers has been detected by various methods (24, 25, 28). ^{29}Si MAS NMR spectra for this family are the same regardless of stacking sequence indicating that the local environment is invariant for all members of the family (46). ZSM-5 and ZSM-11 are end members of the pentasil family which vary only by the stacking sequence of layers, where neighbouring layers are related by inversion or reflectance. High field (9.4T) ^{29}Si MAS NMR spectra (46) of highly dealuminated samples (Fig. 6) clearly reflect the uniqueness of the ZSM-5(7) and ZSM-11 structures and demonstrate that the sequence of layers considerably alters the local T-atom environments. The resolution of the ZSM-5 ^{29}Si MAS NMR spectrum has been considerably improved in recent experiments so that 21 lines can be clearly observed with a resolution of -0.01 ppm (47), again indicating 24 independent T-atoms.

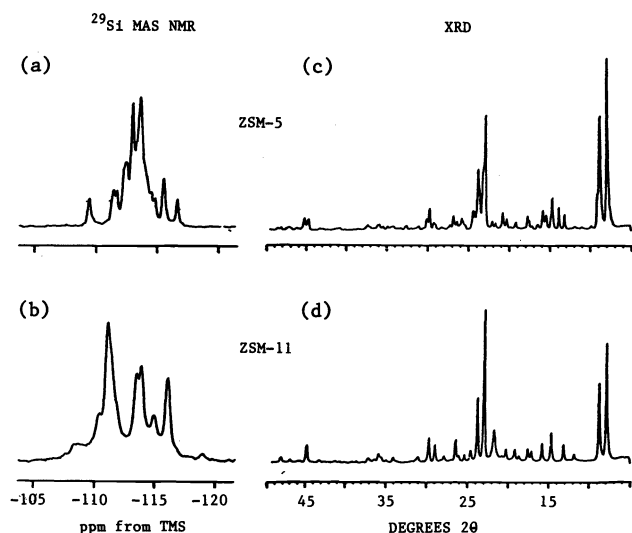


Fig. 6 (a) and (b) The ^{29}Si MAS NMR spectra obtained at 9.4T of samples of highly siliceous ZSM-5 and ZSM-11 respectively, prepared by hydrothermal dealumination techniques. (c) and (d) The corresponding powder XRD patterns of the same samples.

LINE BROADENING DUE TO LOCAL STRUCTURAL EFFECTS

Since MAS NMR reflects the local nuclear environment, any effects which give rise to a distribution of these environments will give rise to line broadening. This is illustrated in Fig. 7 for ZSM-39. The framework structure was found to be pseudo-face-centered-pseudo-cubic, with ideal symmetry $Fd\bar{3}m$ (12) with a few weak reflections suggesting lower symmetry. The spectra of four different ZSM-39 samples (Fig. 6a-d) show varying degrees of line broadening which cannot be due to Al distribution as the Si/Al ratios for three of the samples is very high and the fourth, Fig. 7d, was synthesized in an aminopropane base (sample courtesy of D.M. Bibby). There are three independent atoms in the ideal $Fd\bar{3}m$ structure, $8T_1$, $32T_2$, $96T_3$, and the three signals in spectrum a can be assigned as indicated. In spectrum b, c and d, the lines narrow and extra resonances are resolved. In spectrum d, $3T_3$ resonances of equal intensity are seen making the relative spectral intensities 1:4:4:4:4. This splitting is due to a rotation about the $[111]$ axis with loss of threefold symmetry. The same distortion is thought to be present in the other samples to varying degrees but is uncorrelated throughout the crystals giving a distribution of local environments and consequent line broadening. The XRD patterns of the four structures are very similar and the use of the two techniques together results in a more complete description of the structures (48).

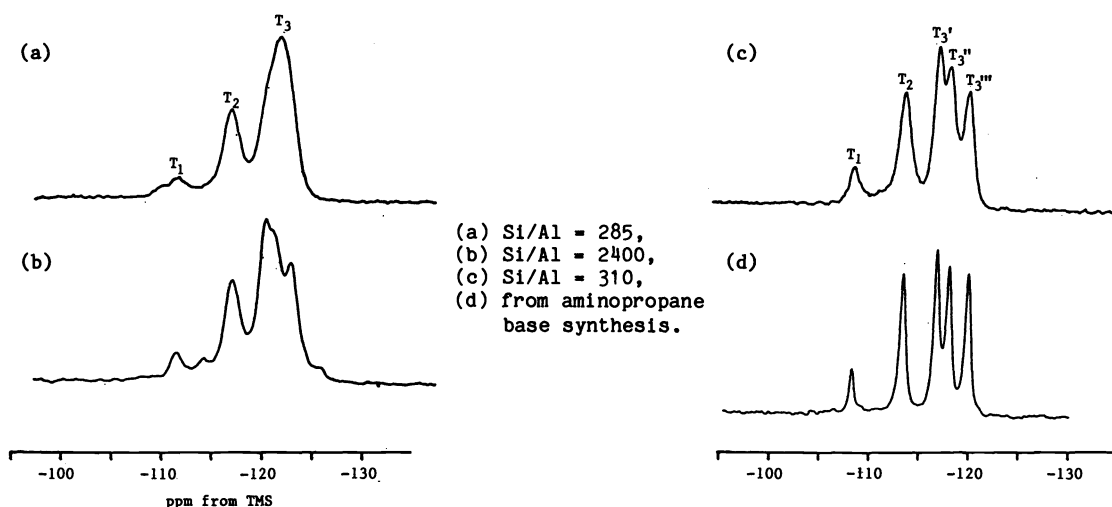


Fig. 7 ^{29}Si MAS NMR spectra of zeolite ZSM-39 with differing Si/Al ratios;

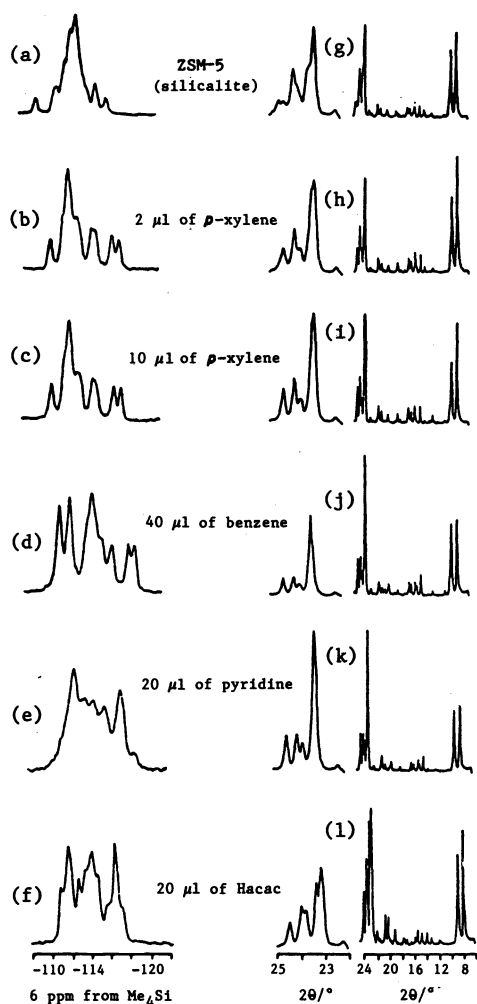


Fig. 8

Fig. 8 ^{29}Si MAS NMR spectra of highly siliceous ZSM-5 and this material treated with various organic molecules (a-f), as well as the corresponding powder XRD patterns (g-l).

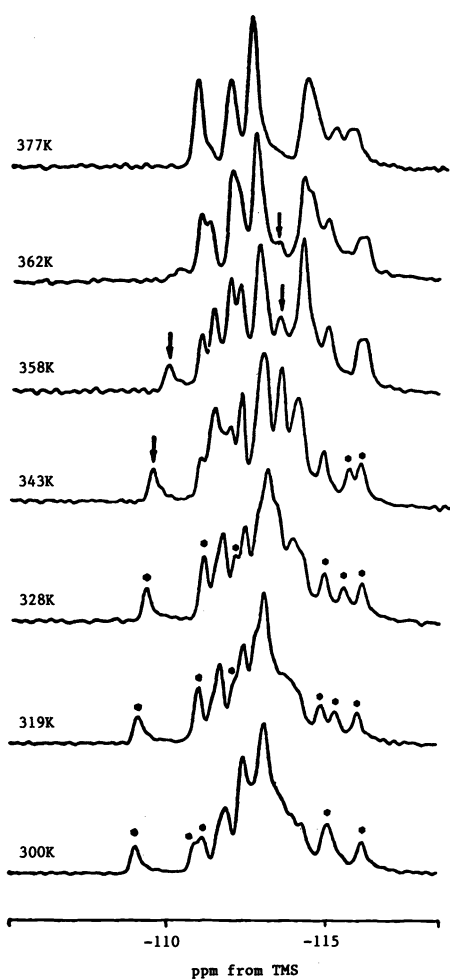


Fig. 9

Fig. 9 ^{29}Si MAS NMR spectra of highly siliceous ZSM-5 at the indicated temperatures.

EFFECT OF SORBED ORGANIC MOLECULES

The ^{29}Si MAS NMR spectra of dealuminated ZSM-5 and ZSM-11 are modified by the sorption of small quantities of organic molecules with related changes in the corresponding XRD patterns (49) confirmed independently by West (51). The limiting spectra, Fig. 81 are characteristic of the sorbed organic molecule. As the concentration of the sorbate is increased, gradual changes are observed until a critical concentration is reached where there is an abrupt change over a small concentration range to the limiting spectrum (52) which does not change further except to lose resolution. The XRD patterns indicate an initial change from monoclinic to orthorhombic symmetry with the loss of the characteristic doublet at $24.4^\circ 2\theta$ and then changes in the lattice parameters are reflected by the XRD lines in the $23 - 25^\circ 2\theta$ range in agreement with NMR data. This indicates that structural changes are occurring which are characteristic of the sorbate while the integrity of the framework is maintained. These changes are completely reversible on desorption and no effects are observed from molecules which are too large to enter the lattice.

EFFECT OF TEMPERATURE

The structure of highly siliceous ZSM-5 is also affected by temperature (53, 54). ^{29}Si MAS NMR spectra obtained at 5° intervals in the temperature range 300-377 K (some shown in Fig. 9) indicate gradual changes with movement of some resonances as indicated culminating in a discrete change between 355 and 365 K where there is a monoclinic to orthorhombic phase transition. These results are in agreement with X-ray data except that the phase transition is detected at a lower temperature (54). The effect is again reversible. The addition of a sorbate such as acetylacetone tends to lower the temperature at which the phase transition takes place if the amount sorbed is below that required for a sorbate induced phase transition. The ^{29}Si MAS NMR spectra for ZSM-5 with ~ 2.4 acac molecules per unit cell sorbed shows a change in the overall profile. There is a very discrete transition over a very small temperature range (323 - 328 K) in which resonances disappear and new ones appear rather than a gradual shift. Above this temperature there are only small and gradual shifts reflecting gradual changes in the local environment of nuclei. Spectra of samples loaded with ~ 4.1 acac molecules per unit cell which is higher than required for a sorbate induced phase transition have profiles of the temperature effect characterized by gradual changes over the 300 - 367 K range.

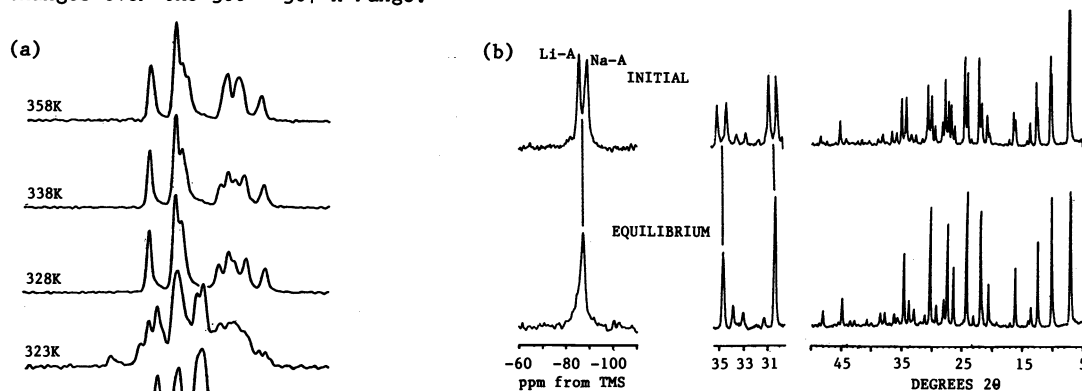


Fig. 10

a) ^{29}Si MAS NMR spectra of dealuminated ZSM-5 with $4.3 \mu\text{l}/100 \text{ mg}$ acac (2.4 molecules/unit cell) sorbed at indicated temperature.

b) ^{29}Si MAS NMR spectra of a mixture of LiA and NaA immediately after mixing and after 10 seconds in a "wiggiebug" together with their corresponding XRD powder patterns.

ION MOBILITY IN ZEOLITES

The rapid inter and intra particle migration of cations between different zeolite crystals due to simple mechanical contact has been demonstrated by ^{29}Si MAS NMR and X-ray powder data. ^{29}Si MAS NMR can distinguish between LiA and NaA. If these two fully hydrated zeolites are mixed for 10 seconds a single species results as seen from NMR and XRD data. Fig. 10b, indicating a very fast ion migration between crystallites. The reaction is dependent on the degree of mixing, the water content and the crystallite size of the zeolite.

Acknowledgements

The authors would like to acknowledge the financial support of the Natural Sciences and Engineering Research Council (Canada) in the form of Operating and Strategic Grants (CAF) and Graduate Fellowships (G.C.G., G.J.K.). One of us (GTK) acknowledges the Alexander Von Humboldt Sr US Scientist Award.

REFERENCES

1. R.M. Barrer, Zeolites and Clay Minerals as Sorbents and Molecular Sieves, Academic Press, N.Y., 1978.
2. J.W. Ward, J. Catal., **13**, 321, 1969.
3. J.A. Rabo, Catalysis by Zeolites, Elsevier, Amsterdam, 1980.
4. P.A. Jacobs, Carboniogenic Activity of Zeolites, Elsevier, Amsterdam, 1977.
5. Ch. Baerlocher, A. Hepp and W.M. Meier, DLS 76, A Program for Simulation of Crystal Structures by Geometric Refinement, Zurich, Switzerland, 1977.
6. D.K. Smith, Revised Program for Calculating X-ray Power Diffraction Patterns UCRL 502.64 Lawrence Radiation Lab, 1967.
7. G.T. Kokotailo, S.L. Lawton, D.H. Olson and W.M. Meier, Nature **272**, 437, 1978.
8. G.T. Kokotailo, P. Chu, S. Lawton and W.H. Meier, Nature, **275**, 119, 1978.
9. R.B. LaPierre, A.C. Rohrman, J.S. Schlenker, J.D. Wood, M.V. Rubin, and W. J. Rohrbaugh, Zeolites, **5**, 346, 1985.
10. G.T. Kokotailo, J.L. Schlenker, F.G. Dwyer and E.W. Valyocsik, Zeolites, **5**, 349, 1985.
11. A.C. Rohrman, R.B. LaPierre, J.L. Schlenker, J.D. Wood, E.W. Valyocsik, M.K. Rubin, J.B. Higgins and W.J. Rohrbaugh, Zeolites, **5** 352, 1985.
12. J.L. Schlenker, F.G. Dwyer, E.E. Jenkins, W.J. Rohrbaugh, G.T. Kokotailo and W.M. Meier, Nature, **294**, 340, 1981.
13. S.A.I. Barri, G.W. Smith, D. White and D. Young, Nature, **312**, 533, 1984.
14. W.M. Meier, Soc. Chem. Ind. 1968, p10.
15. D.W. Breck, Zeolite Molecular Sieves, John Wiley and Sons, N.Y., 1974.
16. R. Von Ballmoos and W.M. Meier, Nature, **289**, 78, 1981.
17. T.J. Weeks, Jr. and D.E. Passoja, Clays and Clay Minerals, **25**, 211, 1977.
18. W.J. Mortier, Compilation of Extra Framework Sites in Zeolites, Butterworth, London, 1982.
19. H.M. Rietveld, J. Appl. Cryst. **2**, 65, 1969.
20. L.B. McCusker and Ch. Baerlocher, Proc. Sixth Int. Conf. Zeolites, Reno, 1983.
21. P. Eisenberger, J.B. Newsam, M.E. Leonowicz and D.E.W. Vaughan, Nature, **309**, 45, 1984.
22. J.M. Bennett, D.E. Cox and C.S. Blackwell, J. Phys. Chem. **87** 3783, 1983.
23. K.L.M. Minachev, G.V. Antoshin, E. Spiro, and H. Isakov, Izv. Akad. Nauk., SSSR. Serkhim. 2131, 1973.
24. J.M. Bennett and J.A. Gard, Nature, **214**, 1005, 1967.
25. G.T. Kokotailo, S. Sawruk and S.L. Lawton, Am. Mineral. **57**, 439, 1972.
26. S. Sawruk, A.C. Rohrman and G.T. Kokotailo, Proc. Fifth Int. Zeolite Conf., Naples, 1980, supplement.
27. G.T. Kokotailo, J.L. Schlenker, Adv. X-ray Anal., **24**, 49, 1981.
28. J.M. Thomas, Proc. Fifth Int. Conf. on Catal., Berlin, 1984, Verlag Chemie Vol 1, p31.
29. A complete description of the various solid NMR techniques and their chemical applications has been presented in "Solid-State NMR for Chemists", C.A. Fyfe, C.F.C. Press, Guelph (1984).
30. E.R. Andrew, A. Bradbury and R.G. Eades, Nature, **182**, 1659, 1958.
31. A. Pines, M.G. Gibby and J.S. Waugh, Chem. Phys. L. **15**, 237, 1972.
32. J. Schaefer and E.O. Stejskal, J. Am. Chem. Soc., **98**, 1031, 1976.
33. E. Lippmaa, M. Magi, A. Samoson, M. Tarmak, and G. Engelhardt, J. Am. Chem. Soc., **103**, 4992, 1981.
34. C.A. Fyfe, J.M. Thomas, J. Klinowski and G.C. Gobbi, Angew. Int. Ed. Engl. **22**, 259, 1983.
35. C.A. Fyfe, G.C. Gobbi, G.J. Kennedy, J.D. Graham, R.S. Ozubko, W.A. Murphy, A. Bothner-By, J. Dadok and A.S. Chesnick, Zeolites, **5**, 179, 1985.
36. G.T. Kerr, J. Phys. Chem., **71**, 4155, 1967.
37. C.A. Fyfe, G.J. Kennedy, G.T. Kokotailo, C.T. DeSchutter, J. Chem. Soc., Chem. Commun. 1093, 1984.
38. C.A. Fyfe, G.C. Gobbi, W.J. Murphy, R.S. Ozubko and D.A. Slack, J. Am. Chem. Soc., **106**, 4435, 1984.
39. L.M. Parker and D.M. Bibby, Zeolites, **3**, 8, 1983.
40. C.A. Fyfe and G.T. Kokotailo (submitted).
41. F. Liebau, Personal Communication.
42. U.S. Patent 3,832,449.
43. U.S. Patent 4,076,842.
44. Eur. Patent. Appl. 0055046.
45. U.S. Patent 3,308,069.
46. G.T. Kokotailo, C.A. Fyfe, G.C. Gobbi, G.J. Kennedy, G.T. DeSchutter, R. S. Ozubko, and W.J. Murphy, Zeolites **85**, Elsevier, Amsterdam, Ed. B. Drzai, D. Hocevar and S. Pjenovik.
47. C.A. Fyfe and H.J. Strobl, submitted.
48. G.T. Kokotailo, C.A. Fyfe, G.C. Gobbi, G.J. Kennedy and C.T. DeSchutter, J. Chem. Soc., Chem. Commun., 1208, 1984.
49. C.A. Fyfe, G.J. Kennedy, C.T. DeSchutter and G.T. Kokotailo, J. Chem. Soc., Chem Commun., 541, 1984.
50. G.J. Kennedy, Thesis, University of Guelph, 1985.
51. G.W. West, Aust. J. Chem. **37**, 455, 1984.
52. C.A. Fyfe, G.T. Kokotailo, G.J. Kennedy, and C.T. DeSchutter, unpublished data.
53. a) C.A. Fyfe, G.T. Kokotailo, G.J. Kennedy, H.J. Strobl and W.W. Fleming, submitted.
b) C.A. Fyfe, G.T. Kokotailo, G.J. Kennedy, J.R. Lyerla and W.W. Fleming, J. Chem. Soc. Chem. Commun. 740, 1985.
54. D.G. Hay, and H. Jaeger, J. Chem. Soc., Chem Commun., 1433, 1984.
55. C.A. Fyfe, G.T. Kokotailo, J.D. Graham, C. Browning, G.C. Gobbi, M. Hyland, G.J. Kennedy and C.T. DeSchutter, J. Amer. Chem. Soc. **108**, 522 (1986).